

# Diffusion of nitrogen gas through polyethylene based films

Annamaria Visco<sup>1,2</sup>  | Cristina Scolaro<sup>1</sup>  | Alfio Torrisi<sup>3</sup>  | Lorenzo Torrisi<sup>4</sup> 

<sup>1</sup>Department of Engineering, University of Messina, Messina, Italy

<sup>2</sup>Institute for Polymers, Composites and Biomaterials - CNR IPCB, Catania, Italy

<sup>3</sup>Department of Mathematics and Physics "Ennio De Giorgi", CEDAD (Center of applied physics, DAting and Diagnostics), Lecce, Italy

<sup>4</sup>Department of Mathematics and Computer Sciences, Physical Sciences and Earth Sciences, MIFT, Università di Messina, Messina, Italy

## Correspondence

Annamaria Visco and Cristina Scolaro, Department of Engineering, University of Messina, Messina, Italy.  
Email: annamaria.visco@unime.it and cristina.scolaro@unime.it

## Funding information

University of Messina Research & Mobility 2016–2019 Project, Grant/Award Number: 74893496

## Abstract

Polyethylene-based films can be used as sealant materials at room temperature in packaging applications. They can be also melted and sealed with glass, acting as sealant material in solar cells. The polyethylene-based polymers investigated in this paper are a linear low-density polyethylene modified with maleic anhydride (or PE-MAH), and an ethylene acrylic acid copolymer (or EMAA). Measurements of nitrogen gas diffusion coefficient (D) have been performed at three different temperatures ranging between 23°C and 32°C. The experimental apparatus used to measure the diffusion coefficients is original compared with other commonly used. The obtained D results have been correlated with the polymeric structure and morphology by means of differential scanning calorimetry (DSC), thermogravimetric-analyses (TGA), X-ray diffraction (XRD), and scanning electron microscopy (SEM) experimental analyses. Furthermore, D-coefficients are compared with the literature data of other polyethylenes with different structural organization (HDPE, LLDPE, and LDPE). The thermal activation energy is evaluated for the two polymers. Arrhenius plot has been used to calculate the activation energies of both polymers and to predict the D-coefficient at other temperatures, close to these analyzed.

## KEYWORDS

activation energy, diffusion coefficient calculation, nitrogen diffusion, polyethylene, polymeric structure

## 1 | INTRODUCTION

Among all the polymers, polyethylene has been widely studied from several points of view due to its high flexibility, strength, easy of processing, transparency, lightweight, and versatility for the various industrial sectors of application, from simple objects of everyday life to prostheses used in the biomedical field, pure and combined in nanocomposites.<sup>1–4</sup>

In packaging or sealants applications, is very important to know the gas permeability features of polyethylene film.<sup>5,6</sup> This controls the quality of food and its preservation during storage and throughout the distribution chain in order to ensure the quality of the product until it reaches the consumer.<sup>7</sup>

The diffusion of small molecules into polymer is mainly function of the polymer structure, diffusing species, temperature, and applied concentration gradient.<sup>8</sup> Thus, a significant role is given to the molecular size and shape of the solute, to the morphology and structure of the polymer, to the solubility limit of the solute in the polymer, to the volatility of the solute and the surface energies of the solid–gas interfaces.<sup>9</sup> In particular, the diffusion coefficient of gasses in polymers increases with the temperature and decreases when the molecular size and the polymer viscosity are increased.<sup>10,11</sup>

Solid polymers have high viscosity at room temperature,<sup>12</sup> generally above 10<sup>12</sup> Pa·s, which is dependent on the stress applied to the polymer and the polymer density. In dense polymers, the diffusion process through the solid is strongly reduced, especially for large

This is an open access article under the terms of the Creative Commons Attribution License, which permits use, distribution and reproduction in any medium, provided the original work is properly cited.

© 2021 The Authors. *Polymer Crystallization* published by Wiley Periodicals LLC.

**TABLE 1** Some nitrogen diffusion coefficients in different density polyethylene polymers at two temperatures

Polymer	T[°C]	D[x10 <sup>-7</sup> cm <sup>2</sup> /s]
LDPE (Low density polyethylene)	70	20
	80	24
MDPE (Medium density polyethylene)	70	11
	80	16
HDPE (High density polyethylene)	70	12
	80	10

molecules, but it can be increased enhancing the temperature and the applied stress.<sup>13</sup> As an example, Table 1 lists some nitrogen diffusion coefficients in different density polyethylene polymers as a function of the temperature<sup>8</sup>:

The nitrogen diffusion coefficients are of the order of 10<sup>-7</sup> cm<sup>2</sup>/s and appear very low also at temperatures up to 80°C, indicating that these polymeric structures are not very permeable to this gas and are less permeable to heavy species such as CO<sub>2</sub>.

Linear-low-density-polyethylene (LLDPE) is usually used as a food protection film (or barrier films) for vacuum and non-vacuum packaging, to prevent contamination, oxidation, and other infiltration of contaminants.<sup>7</sup> In our previous paper, we considered this polyethylene useful as glass sealant material, for solar cells. We studied an LLDPE-maleic anhydride (Bynel<sup>®</sup>, codified as PE-MAH) and an ionomeric LLDPE-methacrylic acid copolymer (Surlyn<sup>®</sup>, codified as EMAA).<sup>14,15</sup> Functional groups (maleic anhydride and methacrylic acid copolymer) in LLDPE provide an adhesive power toward the two glass counterparts. We explored the adhesion power of the two adhesives by means of a mechanical static test, and the wet ability with water at different temperatures (30°C and 80°C). Thus, we proved that PE-MAH have a good adhesive power with glass, and water impermeability than EMAA.<sup>16,17</sup>

In the present paper, we investigated the nitrogen gas diffusion coefficients in both the PE-MAH and EMAA DuPont polymer adhesives at different temperatures (range 23°C–32°C). We present an original instrumentation with respect to others commonly used in literature projected and developed in the Physics laboratory of MIFT of Messina University. The experimental method used to measure the N<sub>2</sub> diffusion coefficient is innovative, simple, and accurate compared with others used in the literature.<sup>18–21</sup> This is because it is based on the application of a known pressure gradient (the two faces of the polymeric film are subjected to a pressure of 2 bar in one face and a dynamic vacuum in the other). The high stress applied on a surface of 20 mm<sup>2</sup> does not cause the breaking of the film; furthermore, the continuous monitoring of the pressure gradient allows the exact calculation of the number of molecules crossing the film and their flow.

The knowledge of the permeability characteristics of these films is very important because these polymeric films not only can be used as very good sealants, but they must also protect and preserve what is under their coverage, acting as a barrier to the entry of different gas species.

Presented data focalize on the comparison between the nitrogen gas diffusion in PE-MAH and EMAA and were not reported previously

in the literature at the best of our knowledge. Both polymers act as adhesives and their features are evaluated in terms of gas permeability dependence to their chemical and structural composition. The two functionalized LLDPE have been compared between them and the diffusion data were compared with the literature data for other polyethylenes, such as LDPE, LLDPE, and HDPE.

## 2 | EXPERIMENTAL

### 2.1 | Materials

Linear low-density polyethylene (LLDPE) modified with maleic anhydride (PE-MAH) was supplied by DuPont (Bynel 4164, thickness 60 μm). Ethylene acrylic acid copolymer (EMAA) in which the acid groups are partially neutralized with zinc or sodium ions was supplied by DuPont (Surlyn 1702, thickness 25 μm). The chemical formula of the repeating units is described in Figure 1A,C. These polymers were used as a thin micro-metric film. They appear transparent to the visible light, have a uniform thickness and a very flat surface (roughness less than 1 micron).

The Bynel Series 4100 resins (density of 0.93 g/cm<sup>3</sup>, melting point of 127°C, softening point of 110°C) are typical of LLDPE resins with similar density and melt index values.<sup>15</sup>

The Dupont Surlyn 1702 is an ionomer of ethylene acid copolymer. Its density is 0.95 g/cm<sup>3</sup>, the melting point is 94°C and the softening point is 65°C.<sup>14</sup>

### 2.2 | Characterization methods

X-ray diffraction (XRD) experiments were performed using a BrukerD8 Advance diffractometer (Bruker, Karlsruhe, Germany) at room temperature with a Bragg–Brentano theta-2theta configuration and Cu Kα radiation (40 V, 40 mA). The XRD patterns were collected in the range 10°–60° with a step of 0.1°/s. The crystallinity degree (X<sub>c</sub>) has been calculated based on the XRD profiles from the ratio between the crystalline diffraction area (A<sub>C</sub>) and the total area of the diffraction profile (A<sub>T</sub>), namely:

$$X_c = \frac{A_C}{A_T} \quad (1)$$

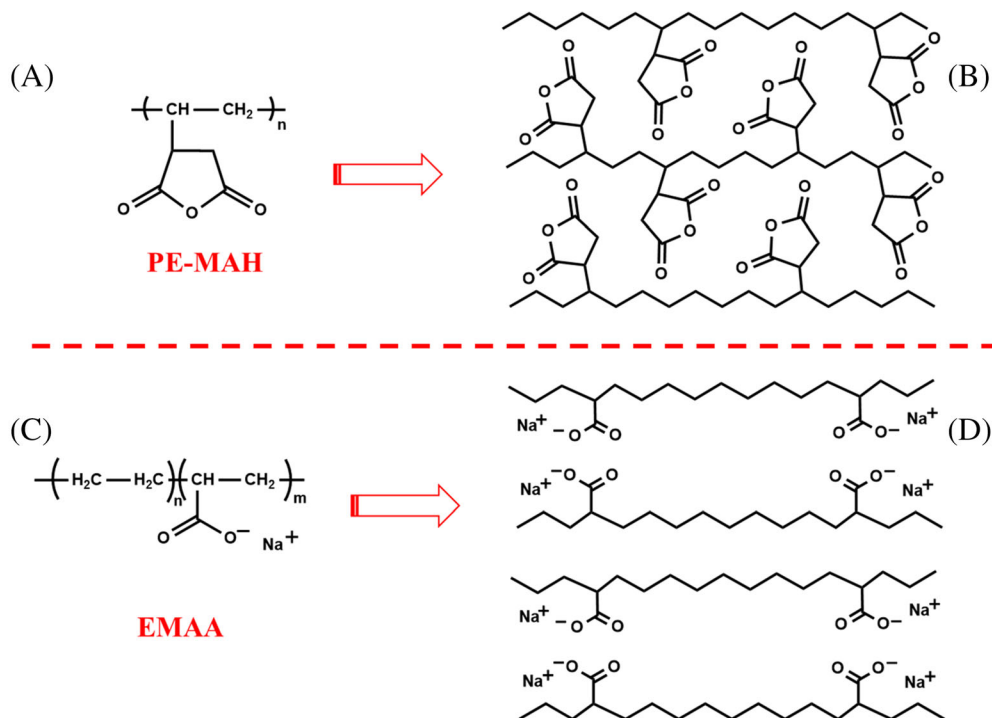
The crystalline diffraction area and that of the amorphous zone were obtained by modeling them respectively as bell peaks on the baseline. Incoherent scattering was taken into consideration.

Differential scanning calorimetry (DSC) was performed using the TAQ500 instrument (TA Instruments, New Castle), under nitrogen flow at a flow rate of 50 ml/min, from room temperature to 230°C, with a heating rate of 10°C/min and water cooling.

DSC analysis let us to calculate the crystallinity degree (%), to conform the data obtained with the XRD analysis by using this formula:

$$X_c (\%) = \frac{\Delta H_c}{\Delta H_m^0} \times 100 \quad (2)$$

**FIGURE 1** Repeating unit (A, C) and polymeric structure (B, D) of PE-MAH and of EMAA



where  $\Delta H_c$  is the enthalpy of the sample under examination,  $\Delta H_m^\circ = 291 \text{ J/g}$  is the melting enthalpy of the theoretical polyethylene 100% crystalline.

Thomson–Gibbs equation has been used to evaluate the polymer's lamellar thickness ( $l_c$ ):

$$l_c = \frac{2\sigma_e}{\rho_c \Delta H_m} \left( 1 - \frac{T_m}{T_m^\circ} \right)^{-1} \quad (3)$$

Where,  $\sigma_e$  or lamellar basal surface free energy is equal to  $9.7 \times 10^{-2} \text{ J m}^{-2}$  is the,  $T_m^\circ$  is equal to  $418.95^\circ\text{K}$  is the extrapolated equilibrium melting temperature of a polyethylene crystal of infinite thickness,  $T_m$  ( $^\circ\text{K}$ ) is the melting peak absolute temperature of polyethylene,  $\rho_c = 1.005 \text{ g cm}^{-3}$ ,  $\Delta H_m = 291 \text{ J/g}$  is the heat fusion per unit volume.<sup>22</sup>

*Thermogravimetric analyses (TGA)* were performed using a TAQ500 instrument (TA Instruments, New Castle) from  $30^\circ\text{C}$  to  $600^\circ\text{C}$ , with a rate of  $5^\circ\text{C}/\text{min}$ , under air and argon flow atmosphere at flow rate of  $100 \text{ ml}/\text{min}$ .

The film morphology, before and after the diffusion measurements, has been observed by *scanning electron microscopy (SEM)* with a FEI Quanta mod. FEG450 (FELMI-ZFE instruments, Graz, Austria). All films adhered on an aluminum holder by means of a graphitic adhesive and were coated by a thin conductive layer before observation. SEM microscope operated with an accelerating voltage of  $3 \text{ kV}$  and in low vacuum mode.

*Diffusion coefficient (D)* measurements of nitrogen gas (molecular weight 28 and kinetic diameter 364 picometers) in PE-MAH and EMAA polymer adhesives were measured by using an original apparatus. It uses a vacuum chamber separated by a high-pressure gas chamber by the thin foil to be investigated.

In this system, the polymeric film, as a thin micrometric foil, is submitted to a strong pressure gradient produced by the nitrogen gas pressure in one face and by the dynamic vacuum conditions ( $10^{-5} \text{ mbar}$ ) in the opposite face. The maximum pressure gradient  $\Delta P/\Delta x$  gradient was about  $80 \text{ mbar}/\mu\text{m}$ .

The nitrogen was admitted in a little know volume  $V_0$  of  $55.8 \text{ cm}^3$  of a reference stainless steel chamber and its pressure  $P_0$  was monitored online with an absolute pressure manometer (Pfeiffer Vacuum Gauge pressure gauge) operating between  $10^{-3}$  and  $3000 \text{ mbar}$ . The temperature  $T_0$  was measured by using a calibrated thermocouple thermally connected to the metallic holder at which the polymer is supported. The polymer holder can be heated from room temperature to about  $100^\circ\text{C}$ .

The accurate measurements of the volume, pressure, and temperature, permitted to evaluate the number of moles admitted in the  $V_0$  reference volume. A calibrated valve at the time zero is opened to permit to the nitrogen gas to arrive at the first face of the polymer film to diffuse through its thickness toward the second face exposed to the high vacuum region. As a function of the time, the gas diffuses in the polymer as a function of the time crossing its thickness and it is removed by the fast vacuum pump system connected to the volume at which the second face is interfaced. Thus, the absolute pressure manometer detects a decrease of the nitrogen gas pressure in the reference volume versus time. A turbo-molecular pump (on which works a mechanical rotary pump) maintains the vacuum conditions at the second face of the polymer at the pressure of  $10^{-5} \text{ mbar}$ . The pressure inside the vacuum chamber is measured by a vacuum gauge. Figure 2 shows a photo (A, C) and a scheme (B) of the used experimental set-up.

The polymer holder was carefully prepared, to expose uniformly the film to the pressure gradient only a small area avoiding high stress and local polymer deformation. Such special holder was projected and

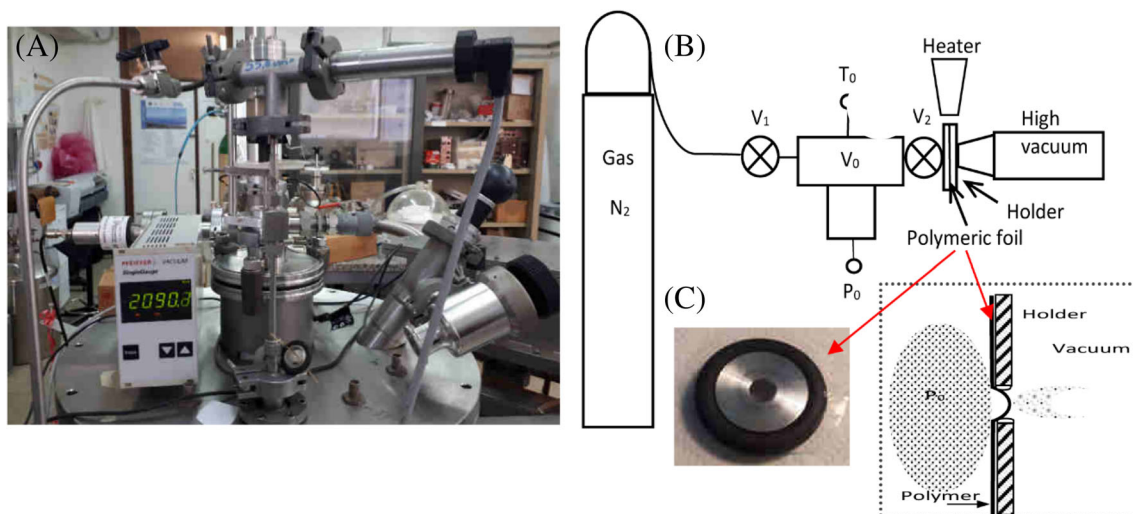


**FIGURE 2** Photo of the experimental set-up (A, C) and scheme of the system and polymer foil holder (B)

realized using a vacuum metallic o-ring holder (Figure 2C); it has a total diameter of 40 mm and a central circular aperture of 5 mm diameter on an aluminum disc of 3 mm thickness, with rounded edges at the contact zones with the film. The gas pressure is applied to a real polymer millimetric surface.

As initial phase the valve  $V_1$  is closed and the valve  $V_2$  is opened to a bypass to the vacuum chamber to produce high vacuum in the  $V_0$  reference volume; successively the valve  $V_2$  is closed and the reference volume  $V_0$  is in vacuum ( $10^{-5}$  mbar). By opening the valve  $V_1$  with the valve  $V_2$  closed, it is possible to flow the nitrogen gas (or other gasses) in the  $V_0$  reference volume up to the desired  $P_0$  pressure, which is accurately controlled by the absolute manometer. In this way, we can calculate the gas concentration in the  $V_0$  reference volume:

$$C_0 = \frac{N_0}{V_0} = \frac{P_0}{kT_0} \quad (4)$$

where  $N_0$  is the initial number of molecules introduced in the  $V_0$  reference volume.

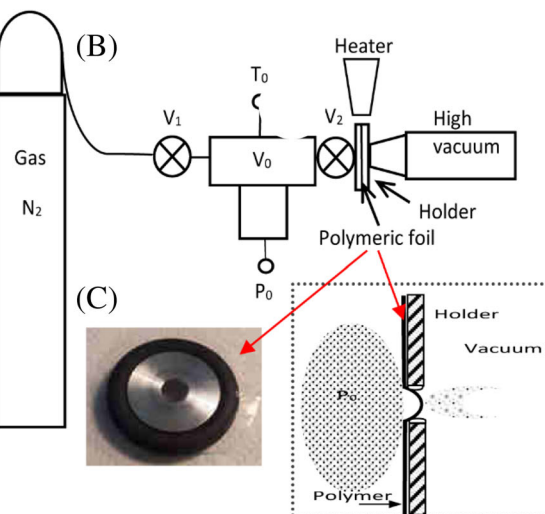
Now, by closing the valve  $V_1$  and opening the valve  $V_2$  the gas flows toward the polymer and diffuses slowly through it up to the vacuum chamber.

The diffused gas in a given time ( $\Delta t$ ) will produce a decrease of pressure  $P_0$  in the small reference chamber  $V_0$ , called  $\Delta P$ . Thus, the number of molecules  $N$  diffused through the polymer can be calculated by the equation:

$$N = \frac{\Delta P V_0}{kT_0} \quad (5)$$

The diffusion coefficient can be calculated by the relation:

$$D = \frac{N}{S \cdot \Delta t} \cdot \frac{\Delta x}{C_0} \quad (6)$$



The  $N_2$  molecules diffuse through a polymer surface  $S = 19.63 \text{ mm}^2$ , which was evaluated  $20 \text{ mm}^2$  due to the small tensile deformation under the pressure gradient (see Figure 2D), flowing for a time  $\Delta t$  from the valve  $V_2$  aperture, under the concentration gradient  $C_0/\Delta x$ .

An electrical heater (resistor) applied to the holder was used to change the polymer temperature from room temperature ( $23^\circ\text{C}$ ) up to  $32^\circ\text{C}$ . Test of gas diffusions were performed with  $N_2$  pure gas.

To highlight the different behavior of the two polymers studied with respect to the temperature, it is possible to refer the results to the Arrhenius graph to analyze the effect of temperature on the nitrogen diffusion rates. In this diagram, the logarithm of the diffusivity ( $\ln(D)$ ) is plotted versus the reciprocal absolute temperature ( $1000/T$ ).

The diffusivity coefficient depends on the temperature according to an activation energy  $\Delta E$  promoting the diffusivity process, following the exponential law<sup>23</sup>:

$$D = D_0 \cdot e^{-\frac{\Delta E}{kT}} \quad (7)$$

where  $D_0$  is the maximum diffusivity value,  $k$  is the Boltzmann constant,  $T$  is the absolute temperature (K). This equation can be written as:

$$\ln(D) = \ln(D_0) - \frac{\Delta E}{k} \cdot \left(\frac{1}{T}\right) \quad (8)$$

From this relation we can see how the natural logarithm of the diffusion coefficient is proportional to  $1/T$  and that therefore in a diagram  $\ln(D)$  versus  $1/T$ , the pre-exponential factor  $\ln(D_0)$  is equal to the vertical intercept and the slope of the line, which is equal to  $-\Delta E/k$ .

The activation energies of the thermal process can be calculated by measuring the diffusion coefficients at two temperatures by the relation:

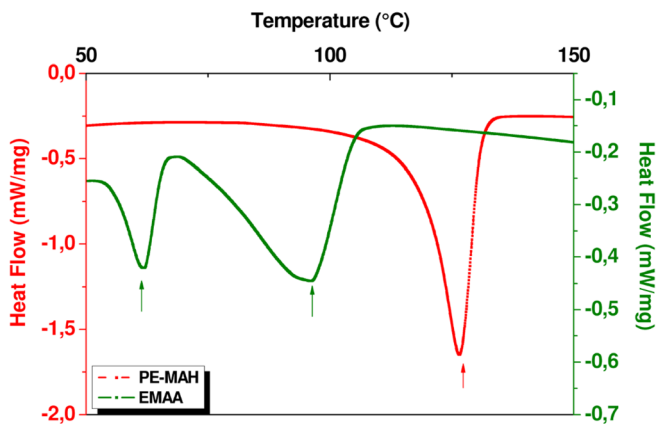


**FIGURE 3** Comparison between the DSC curves of the PE-MAH and EMAA

$$\Delta E = \left( k \cdot \ln \frac{D_1}{D_2} \right) / \left( \frac{1}{T_2} - \frac{1}{T_1} \right) \quad (9)$$

### 3 | DISCUSSION

In this section, the material's characterization is presented and discussed. It has been carried out by means of DSC and XRD analysis, to check the structural order of both films. TGA results highlighted their thermal stability. Then we performed the nitrogen gas diffusion measurements, and we correlated the polymeric structure features of each film to the diffusion results. This information let us to explain the different permeability. Finally, the Arrhenius plot has been used to calculate the activation energy of the nitrogen gas diffusion, and to predict the diffusion value at different temperatures, close to these investigated.

The calorimetric DSC/TGA and XRD analyzes were useful to know the degree of crystalline order of the PE-MAH and EMAA polymeric films. The DSC curves of Figure 3 shows PE-MAH have a single endothermic peak at 125°C. EMAA shows two endothermic peaks much lower than that of PE-MAH, at 53°C and 89°C, respectively, due to its ionic nature.

The PE-MAH film has a degree of crystallinity of 30% since the presence of maleic anhydride limits the movements of the macromolecular chains. The degree of crystallinity of the EMAA is much lower ( $\approx$  3%–11%) because a copolymer has a typically unordered structure.

To confirm the DSC results about the crystalline degree estimation, XRD analysis has been carried out. The diffraction pattern of both films is shown in Figure 4 where the XRD pattern of LLDPE is presented as reference material. The peaks at 20.7° and 23.8° are the diffraction signals assigned to the polyethylene phase.<sup>24</sup> These peaks appear in the XRD pattern of LLDPE and PE-MAH while are not well defined in EMAA where broad area appears due to its disordered organization that makes very difficult to define the very poor crystalline phase. Furthermore, a quantitative analysis of the XRD peaks indicates a value of about 34% of crystalline order in PE-MAH,

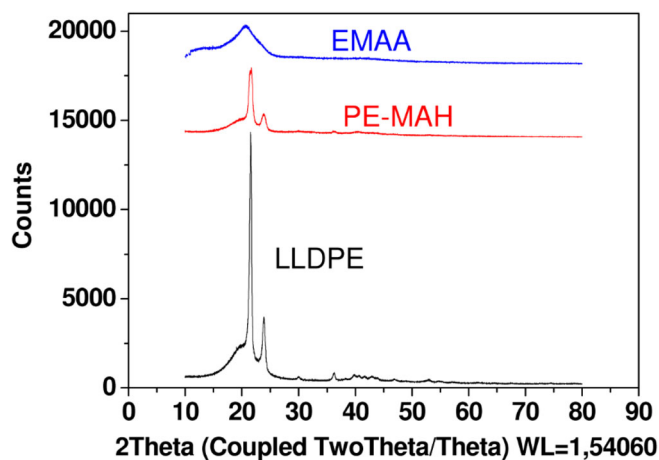


**FIGURE 4** XRD curves of EMAA, PE-MAH, and LLDPE, as reference material

and < 10% in EMAA. Thus, XRD results agree with the calorimetric data as PE-MAH has the highest peak resolution due to a higher crystalline order.

The lamellar thickness of the PE-MAH film (14.54 nm calculated by considering that  $\Delta H = 87.7$  J/g) is higher than that of EMAA (3.01–4.94 nm calculated by considering that  $\Delta H = 8.02$ –32.6 J/g). This suggests that PE-MAH is made up of crystals that are larger in shape and more abundant in quantity than EMAA. These structural characteristics could be related to the different barrier characteristics to gas penetration of the two films, discussed later (Figure 8 and Table 2).

Figure 5 shows the TGA curves of the films, performed in inert environment (Figure 5A) and in air (Figure 5B). In inert environment, PE-MAH starts its decomposition at about 420°C and it shows a single decomposition peak at 490°C. EMAA starts its decomposition earlier than PE-MAH (at about 350°C); it shows a wider decomposition peak than PE-MAH since it contains inside two peaks (at about 460°C and 480°C), due to its copolymeric nature and in agreement with DSC analysis (Figure 5A).

In air both materials decompose earlier than in inert environment (after about 250°C, up to about 530°C), as expected, giving several peaks which represents the different oxidative degradation products. EMAA starts its decomposition earlier (at about 180°C) and faster than PE-MAH (Figure 5B).

Thus, both films exhibit stability until around 400°C in inert and around 200°C in air, and PE-MAH is more stable than EMAA in both environmental conditions.

The nitrogen gas pressure versus time of the two investigated polymers at 23°C (room temperature) is shown in Figure 6A. The measurements of pressure in the  $V_0$  reference gas camera were recorded as a function of the time from the valve  $V_2$  aperture, for a given polymer at a fixed temperature.

It is evident that the EMAA polymer shows a significant diffusion process because the gas pressure in the reference chamber decreases and reduces of about 0.4% after 90 min. The PE-MAH polymer,

Polymeric film code	$X_c$ [%]	$D$ [ $\times 10^{-7}$ cm <sup>2</sup> /s]			
		$T = 23^\circ\text{C}$	$T = 27^\circ\text{C}$	$T = 32^\circ\text{C}$	$T = 69^\circ\text{C}$
PE-MAH	30	0.01	0.8	114	-
EMAA	3–11	5	50	750	-
HDPE <sup>5</sup>	66	-	-	-	12
LDPE <sup>24</sup>	32	0.5	-	-	-
LLDPE <sup>24</sup>	40	0.77	-	-	-
HDPE <sup>24</sup>	56	0.91	-	-	-

**TABLE 2** Crystalline degree ( $X_c$ ) and nitrogen diffusion coefficients ( $D$ ) in the two investigated polymers at 23°C and 32°C, and comparison with other polyethylenes<sup>5,25</sup>

instead, does not show diffusing effect because the pressure in the reference chamber remains constant for 90 min examination. Thus, as a first observation, the nitrogen diffusion coefficient in the EMAA polymer is higher than in the PE-MAH polymer.

Increasing the polymer temperature to 32°C the process of diffusion is more evident and both polymers become more permeable to the nitrogen gas, as shown by the data reported in Figure 6B.

In this case, both polymers show a significant pressure reduction with the diffusion time which was evaluated at 38.5% in the EMAA polymer, 25 microns in thickness, and 2.4% in the PE-MAH, 60 microns in thickness. This result indicates that the nitrogen gas diffusion in the two polymers is growing with the temperature but that their structure is very different because with only 9°C temperature increase the EMAA is quickly shoots to be permeated by the gas.

In all the films of PE-MAH and EMAA analyzed at 23°C, 27°C, and 32°C, it is possible to evaluate the diffusion coefficient ( $D$ ) by using the Equation (6). This procedure gives the values of  $D$  with the values of crystalline degree ( $X_c$ ) listed in the Table 2.

The measurements of  $D$ -coefficients of nitrogen in EMAA are always much higher with respect to that in PE-MAH regardless the temperature value, according to the plots of Figure 6.

Moreover, Table 2 compares the obtained results (first two lines) with that reported in the literature (last four lines), relative to different polyethylene at different densities (such as HDPE, LLDPE, and LDPE). At room temperature (23°C), the diffusion coefficient in PE-MAH resin is the lower. This result could be related to PE-MAH higher crystalline order, and its greater crystallite size compared with EMAA. The diffusion coefficient in EMAA is instead like that in LDPE and higher than the other type of polyethylenes.

Generally, the gas diffusion in thermoplastic polymers grows with increasing the temperature. In fact, as theoretically predicted, N<sub>2</sub> diffusion in the two polymeric adhesives is very low at the room temperature of 23°C in EMAA and negligible in PE-MAH. Afterward, diffusion increases significantly with increasing the temperature of only 9°C (at 32°C). In details, it grows of about four orders of magnitude in PE-MAH (114  $\times 10^{-7}$  cm<sup>2</sup>/s) and of about a factor 150 (two orders of magnitude) in the EMAA (750  $\times 10^{-7}$  cm<sup>2</sup>/s), putting in evidence as EMAA polymeric structure highly changes with the temperatures. Thus, the EMAA polymer is more sensitive to the temperature and becomes easily permeable to nitrogen gas just at 32°C under the pressure gradient at about 80 mbar/ $\mu\text{m}$  thickness.

The high-density polyethylene (HDPE) shows a  $D$ -coefficient of  $1.2 \times 10^{-6}$  cm<sup>2</sup>/s at a temperature of 69°C (Table 1), indicating lower nitrogen diffusion according to its “high-order” typical structure.<sup>5</sup> Permeability, diffusion, and solubility of gasses in polymers depend on material's nature and structure.<sup>8</sup> As known, the degree of crystallinity is the most important parameter to consider since crystalline regions act as physical barriers to impede the gas flow.<sup>10</sup> Barriers depend on both macromolecular orientation and the size of the permanent gas molecules.<sup>26</sup> Penetrant molecules must bypass the impermeable obstacles following a more tortuous path; furthermore, crystallites act as cross-linking, restricting the motions of the chains involved in the diffusion process.<sup>5</sup> The higher crystalline degree of HDPE ( $X_c = 56\%$ ) explains its lower nitrogen gas diffusion compared with the others polyethylene ( $X_c = 32\%$  in LDPE and  $X_c = 40\%$  in LLDPE, see data of Table 2). Permeability of gasses and vapors in polyolefins were highly considered in scientific literature for food packaging and for micro porous membranes employed in several applications (such as microfiltration, blood oxygenation and dialysis, and solar cell devices).<sup>5,27</sup>

The actual measurements demonstrated that the diffusion coefficients measured in this paper align with the values presented by the other polyethylenes at various densities, of the order of  $10^{-7}$  cm<sup>2</sup>/s.<sup>16</sup> In details, the measured  $D$ -coefficients correspond to  $1 \times 10^{-9}$  cm<sup>2</sup>/s in PE-MAH and  $5 \times 10^{-7}$  cm<sup>2</sup>/s in EMAA, for their different crystalline order. PE-MAH, in fact, has a lower crystalline degree than LLDPE ( $X_c = 30\%$  and  $40\%$ , respectively) and EMAA has the lowest one ( $X_c = 3\text{--}11\%$  or, more generally, lower than  $10\%$  that is within the experimental error as suggested by XRD analysis) because of its copolymeric nature of [poly (ethylene-co-methacrylic acid)].

The lower crystalline degree of PE-MAH and EMAA with respect to LLDPE is due to the functional group presence and to their typical polymeric structure shown Figure 1B,D. In PE-MAH polymer (Figure 1B), the wide functional group of maleic anhydride represents a considerable obstacle for the gas diffusion, more than that of the ionomer resin (EMAA) copolymer (Figure 1D) in which are present ionic groups where all the oxygen atoms of carbonyls, negatively charged, repels each other. Consequently, in EMAA the free volume is much higher than in PE-MAH, which is more stable at higher temperatures than EMAA, as suggested by TGA analysis.

For all the above-discussed issues, we could hypotize that a small molecule like that of nitrogen gas (chemical length of N<sub>2</sub> is about 1.1 Å, lower than sp<sup>3</sup> hybridized C-C bond, whose length is of

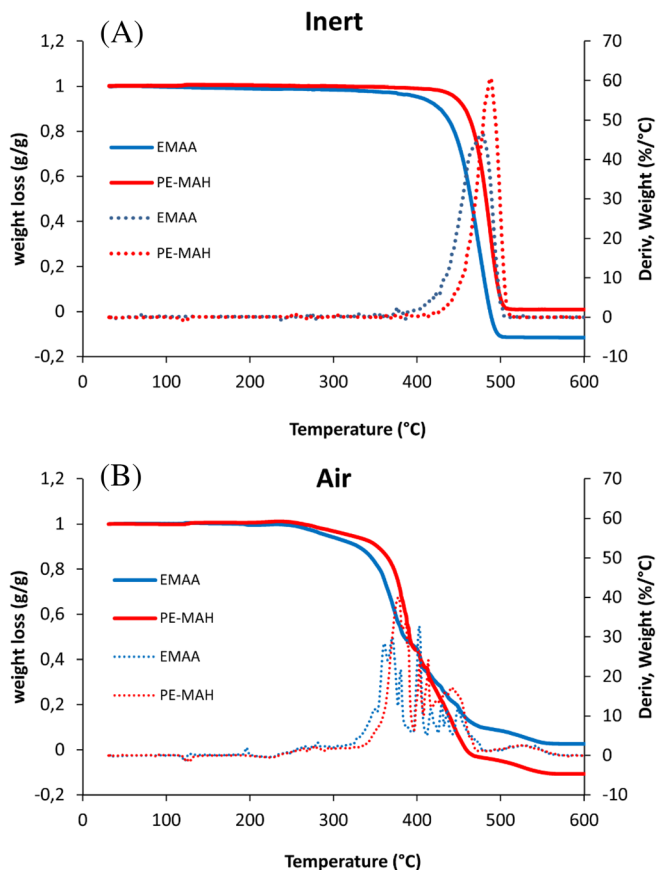


**FIGURE 5** TGA curves of PE-MAH and EMAA, in inert atmosphere (A) and in air (B)

about 1.5°A) takes more time to overcome the large functional pendant groups in PE-MAH with a tortuous path like that represented in Figure 7A. Since EMAA copolymer contains larger spaces (or free volume) due to the high polarity of oxygen atoms in the acrylic functional groups that enlarge the macromolecular chains, it permits to N<sub>2</sub> molecules to get inside with an easier path (Figure 7B).

In order to observe the surface morphology of both films and the changes induced in the two polymeric materials by nitrogen gas diffusion, a SEM investigation has been performed.

Figures 8 and 9 show the SEM images of both films before (A, B) and after the gas diffusion at room temperature (C, D). For each sample there are two images, at low and high magnification, that is, at 10Kx (A, C) and at 350Kx (B, D), respectively. PE-MAH (Figure 8) shows a morphology change after the gas diffusion: the wrinkled surface observed at high magnifications appears smoother (8D) compared with pure sample (8B) and many little damaged areas (or stressed, indicated by the red arrows in the picture) appear in the low magnification morphology (8C).

The micrographs relating to pure EMAA are shown in Figure 9: the low magnification image of the pure film (A) exhibits some depressions and micro-nanoparticles distributed on the surface. EMAA's surface (9B) is much more microrough than PE-MAH (9B). After the diffusion of the gas, EMAA appears much more streaked (with

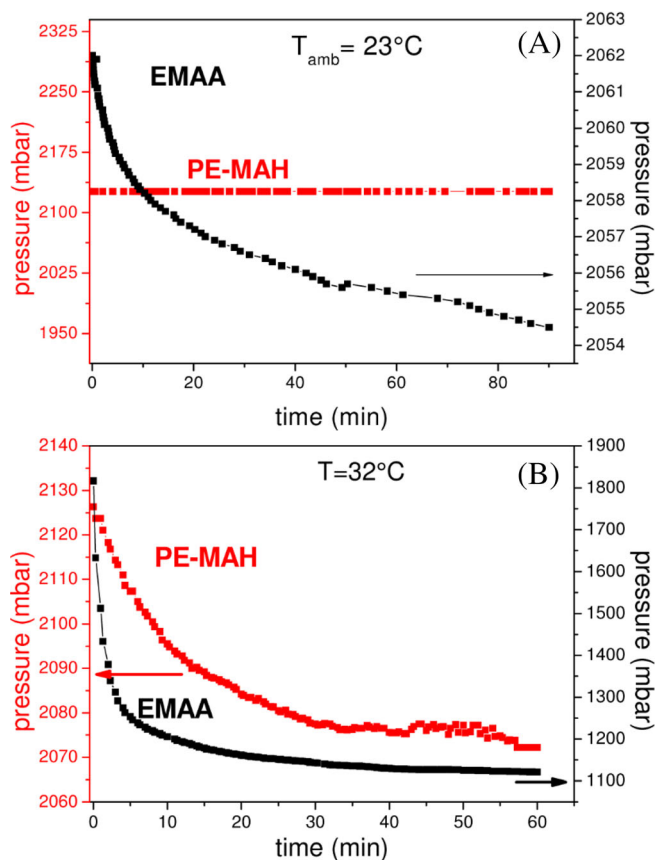


**FIGURE 6** N<sub>2</sub> pressure in the reference volume versus time for the two polymers at 23°C (A) and 32°C (B)

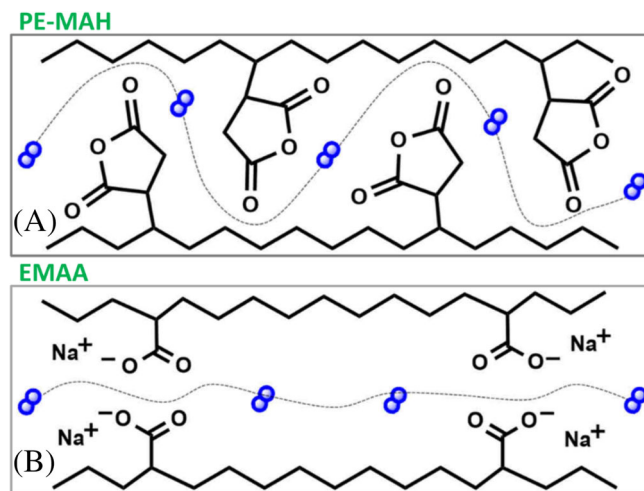


**FIGURE 7** Representation of possible diffusion path of nitrogen gas molecules inside the structure of PE-MAH (A) and of EMAA (B)

superficial stretch marks indicated by the red arrows) (9C) than PE-MAH (8C). This suggests that it has suffered a greater pressure stress than PE-MAH. This stress has left a mark in the material. Thus, PE-MAH (with crystalline degree and crystallite size greater than EMAA) is, therefore, more stable and resistant than EMAA to the pressure

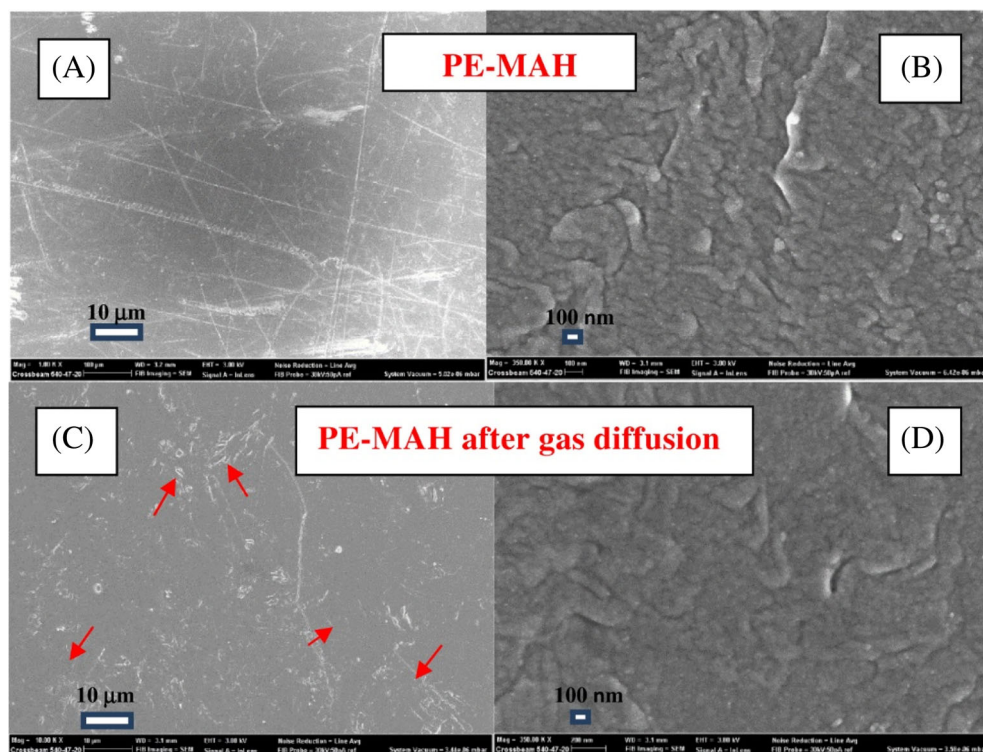


**FIGURE 8** SEM micrographs of PE-MAH film before (A, B) and after the gas diffusion (C, D)

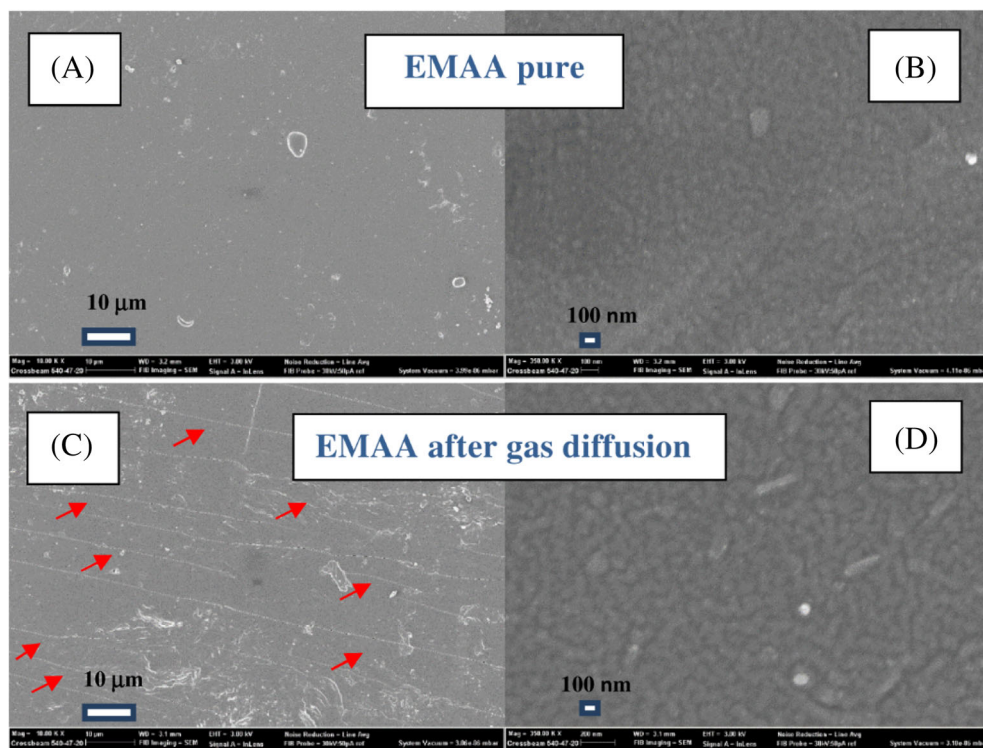


**FIGURE 9** SEM micrographs of EMAA film before (A, B) and after the gas diffusion (C, D)

gradient the nitrogen gas diffusion, in agreement with diffusion results and with TGA results, before discussed. Furthermore, the morphology of EMAA changes as well because elongated morphologies appear at high magnifications (9D), absent without any stress (9B).

Besides, EMAA easily improves, even more, its free volume by raising the temperature, since the ionic groups lose their attraction

forces getting higher mobility than PE-MAH, and leading to the formation of free chains, conferring higher thermal expansion to the material. This can be seen in the graph of Figure 10 which reports the  $N_2$  measured diffusion coefficients in the two investigated polymers as a function of the temperature. The errors of the measurements are within 5%.



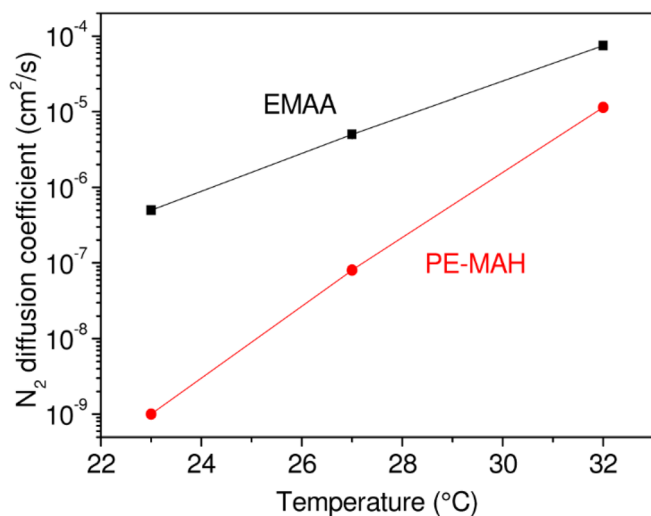


**FIGURE 10** N<sub>2</sub> diffusion coefficient versus temperature for PE-MAH and EMAA

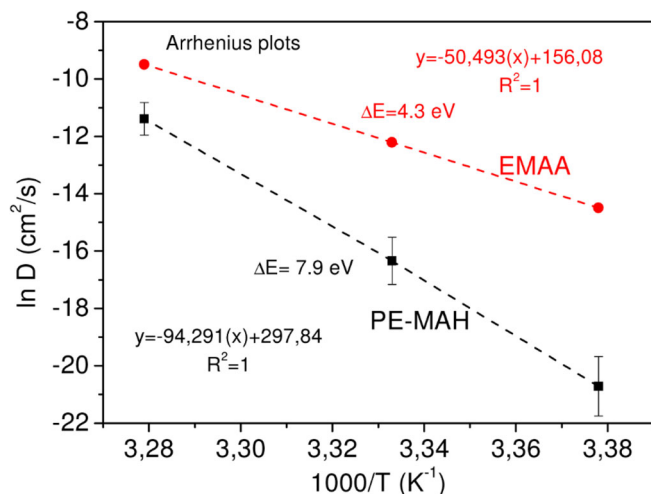


**FIGURE 11** Arrhenius plot with the relative activation energy of PE-MAH and EMAA

Arrhenius plot analyzes the effect of temperature on the rates of nitrogen diffusion.<sup>23</sup> For a single rate-limited thermally activated process, an Arrhenius plot gives a straight line, from which the activation energy and the pre-exponential factor, described by Equation (7) can both be determined. Figure 11 reports our data in the Arrhenius plot relative to the two polymers using Equation (9) versus temperature expressed in the absolute scale and represented as  $1000/T$ . The activation energy measure has demonstrated that the energy to activate the mechanism of diffusion in PE-MAH is about 7.9 eV, a factor 1.7 higher with respect that necessary to activate the diffusion in EMAA (4.6 eV). This result confirms that the EMAA resin is more sensitive to the temperature for the nitrogen diffusion in its structure, according to the data in Figure 7. Instead, PE-MAH is less diffusing material and must be activated with a higher energy, of about a double with respect to the other resin. Thus, the structure of the PE-MAH is more

thermal resistant of the EMAA, in accordance with the results before discussed and with the literature data.<sup>6,9,28</sup>

Using the equations indicated in the graph in Figure 11 we could predict the  $D$  value at different temperatures than those studied, but in a range that is still close. This is because the polymer structure could vary in a nonlinear way with a higher thermal variation, both up and down; this is due to the typical viscoelastic behavior of the polymeric materials.

Literature reports that the apparent activation energies for the diffusion of nitrogen gas in pure polyethylene range between 36 and 46 kJ/mol corresponding to 0.375 and 0.479 eV, respectively.<sup>8</sup> Thus, PE-MAH and EMAA exhibit higher activation energies (7.9 and 4.3 eV, respectively) than pure polyethylene. This result indicates that the polymers investigated in the present research are more stable at room temperature than pure polyethylene and that their diffusion enhancement is less dependent on the temperature increment. This aspect represents an advantage with respect to pure polyethylene, especially for the very low permeable PE-MAH polymer which can be used as a stable sealant for many applications that do not require temperature increases.

As known, diffusion and hence the activation energy, depends on the crystalline order, on the presence of polar and/or hydrophilic functional groups, and on the chemical affinity with the gas.<sup>29</sup> Functional groups such as that in ionomeric resin, and even more maleic group in PE-MAH, could greatly influence the activation energy that results much higher than pure LLDPE.

Therefore, the experimental evidence here presented highlighted as PE-MAH has a higher impermeability to nitrogen gas than EMAA even at higher temperatures as well as a good thermal stability. Indeed, for all these characteristics, PE-MAH films can be used as a sealant with glass in all applications where this type of adhesion is required. For example, in solar cells this film must be vacuum sealed, and must adhere perfectly to the glass to prevent the entry of gaseous species and prevent the oxidation processes of the conductive fluids that are inside or of the semiconductors used for the cell.<sup>14</sup> PE-MAH can also be used as a barrier film in all those applications where thin films must protect the internal content (e.g., food packaging) with stable characteristics over a wide temperature range, up to about 200°C.<sup>30</sup>

## 4 | CONCLUSIONS

In this paper, we have investigated the diffusion of nitrogen, through two polyethylene films, both based on LLDPE employed as sealants layer.

The nitrogen diffusion measurements have been performed within the range 23°C–32°C in a special apparatus.

Results showed that EMAA has a much higher permeability to the gas compared with PE-MAH. With increasing the temperature, the difference between the two materials is less strong: in particular, it's of two magnitude orders at 23°C (from 0.01 to  $5 \times 10^{-7}$  cm<sup>2</sup>/s), of one magnitude order at 27°C (from 0.8 to  $50 \times 10^{-7}$  cm<sup>2</sup>/s) and six times higher at 32°C (from 114 to  $750 \times 10^{-7}$  cm<sup>2</sup>/s).

The activation energy resulted about double in PE-MAH with respect to EMAA, confirming that EMAA is more sensitive to temperature for nitrogen diffusion than PE-MAH. This is due to macromolecular ordered structure of PE-MAH which is much more stable and thermal resistant compared with that of lower crystalline ionomeric EMAA resin, according to literature data. The higher free volume in EMAA structure and, hence, its lower macromolecular chains packaging let an easier nitrogen gas diffusion compared with PE-MAH.

The different structural order reduces the diffusion coefficient of about one order of magnitude: the high diffusivity of nitrogen in EMAA, of  $5 \times 10^{-7} \text{ cm}^2/\text{s}$ , can be due to its low crystallinity, which ranges within 3%–11%. For all the issues above discussed, PE-MAH films exhibit to be more suitable than EMAA ones for sealing applications.

This research lays the foundation for various future insights. Works are in progress to repeat the D-coefficient test at different temperatures, much higher and much lower than those studied in this article, to expand the information on the possible application temperature range and on different gasses. It must be pointed out that we have already experimentally observed that heating these films at a temperature of 80°C under vacuum they completely degrade because they burn off. Such temperature could be considered as a threshold value.

Besides, further permeability investigations are going to be performed by decreasing the gas molecule dimension with respect to nitrogen (i.e., like helium or hydrogen gas) and in films during the degradation in water presence (hydrolysis) or presence of UV light (photo-degradation).

## ACKNOWLEDGMENTS

This research was supported by University of Messina Research & Mobility 2016–2019 Project (project code RES\_AND\_MOB\_2016\_Prof. Lorenzo Torrisi) no.74893496. Authors thanks Dott. Consuelo Celesti and Dott. Amani Khaskhoussi of Engineering Department of Messina University for the helpful discussion, and SEM microscopy observation. Open Access Funding provided by Università degli Studi di Messina within the CRUI-CARE Agreement.

[Correction added on 28 Aug 2021, after first online publication: Funding statement has been added.]

## ORCID

Annamaria Visco  <https://orcid.org/0000-0003-1602-9361>

Cristina Scolaro  <https://orcid.org/0000-0001-5725-9839>

Alfio Torrisi  <https://orcid.org/0000-0003-2404-5062>

Lorenzo Torrisi  <https://orcid.org/0000-0003-0853-136X>

## REFERENCES

- [1] S. W. Kim, Y. H. Chun, *Korean J. Chem. Eng.* **1999**, *64*, 511.
- [2] L. Torrisi, A. M. Visco, N. Campo, F. Caridi, *Nucl. Instrum. Meth. B* **2010**, *268*, 3117.
- [3] M. Catauro, C. Scolaro, G. Dal Poggetto, S. Pacifico, A. Visco, *Polymer* **2020**, *12*, 978.
- [4] A. M. Visco, L. Torrisi, G. Galtieri, C. Scolaro, *J. Thermoplast. Compos. Mater.* **2017**, *30*, 1675.
- [5] L. Kubik, S. Zeman, *Res. Agric. Eng.* **2013**, *59*, 3,105.
- [6] A. Visco, G. Di Marco, C. Scolaro, D. Iannazzo, L. Torrisi, *AIP Conf. Proc.* **1981**, 2018, 020145.
- [7] Y. Wang, A. J. Easteal, X. D. Chen, *Packag. Technol. Sci.* **1998**, *11*(4), 169.
- [8] B. Flaconneche, J. Martin, M. H. Klopffer, *Oil Gas Sci. Technol.* **2001**, *56*(3), 261.
- [9] A. S. Michaels, H. J. Bixler, *J. Polym. Sci.* **1961**, *50*(154), 413.
- [10] M. H. Klopffer, B. Flaconneche, *Oil Gas Sci. Technol.* **2001**, *56*(3), 223.
- [11] D. R. Paul, A. T. Di Benedetto, *J. Polym. Sci., Part C: Polym. Symp.* **1965**, *10*(1), 17.
- [12] M. H. Khaliq, R. Gomes, C. Fernandes, J. Nóbrega, O. S. Carneiro, L. L. Ferrás, *Rapid Prototyp. J.* **2017**, *23*(4), 727.
- [13] Y. Sato, K. Fujiwara, T. Takikawa, S. S. Takishima, H. Masuoka, *Fluid Ph. Equilibria* **1999**, *162*, 261.
- [14] Dupont, Bynel<sup>®</sup> Coextrudable Adhesive Resin, [https://www.google.com/url?sa=t&source=web&rct=j&url=http://dpsp-solutions.com/wp-content/uploads/Dow-DuPont-Bynel-Coextrudable-Adhesive-Resins-ENG.pdf&ved=2ahUKEwik84bzj\\_PwAhUWxBQKHcfZA84QFjAAegQIAxAC&usq=AOvVaw2MKRUJ8EvtznqTXIPnEgu](https://www.google.com/url?sa=t&source=web&rct=j&url=http://dpsp-solutions.com/wp-content/uploads/Dow-DuPont-Bynel-Coextrudable-Adhesive-Resins-ENG.pdf&ved=2ahUKEwik84bzj_PwAhUWxBQKHcfZA84QFjAAegQIAxAC&usq=AOvVaw2MKRUJ8EvtznqTXIPnEgu) accessed: August, 2021
- [15] Surlyn<sup>®</sup> 1702 Datasheet, <http://iigc.mx/Fichas/DuPont-Surlyn-1702.pdf> accessed: August, 2021
- [16] J. F. Medel, F. Garcia-Alvarez, E. Gomez-Barrena, J. A. Pertola, *Polym. Degrad. Stab.* **2019**, *88*(3), 435.
- [17] A. Visco, C. Scolaro, D. Iannazzo, G. Di Marco, *Int. J. Polym. Anal. Charact.* **2019**, *24*(2), 97.
- [18] L. Torrisi, C. Gentile, A. M. Visco, N. Campo, *Radiat. Eff. Defects Solids* **2003**, *158*(10), 731.
- [19] L. Torrisi, A. Ilacqua, F. Caridi, N. Campo, A. Picciotto, R. Barnà, D. De Pasquale, M. Trimarchi, A. Trifirò, L. Auditore, *Radiat. Eff. Defects Solids* **2006**, *161*(1), 3.
- [20] W. Jost, *Diffusion in solids, Liquids and gases*, Academic Press Inc., NJ, USA **1960**.
- [21] K. Haraya, S. T. Hwan, *J. Membr. Sci.* **1992**, *71*(1–2), 13.
- [22] A. R. C. Duarte, C. Martins, P. Coimbra, M. H. M. Gil, H. C. de Sousa, C. M. M. J. Supercrit, *Fluids* **2006**, *38*, 392.
- [23] H. Mehrer, *Diffusion in solids - Fundamentals, Methods, Materials, Diffusion-Controlled Processes*, Springer, Berlin, Heidelberg, New York **2007**.
- [24] M. Ardanuy, J. I. Velasco, M. L. Maspoch, L. Haurie, A. I. Fernandez, *J. Appl. Polym. Sci.* **2009**, *113*(2), 950.
- [25] M. Pino, R. A. Duckett, I. M. Ward, *Polymer* **2005**, *46*(13), 4882.
- [26] V. Compañ, A. Andrio, M. L. López, E. Riande, *Polymer* **1996**, *37*(26), 5831.
- [27] P. P. Kundu, S. Choe, *J. Macromol. Sci. Polymer. Rev.* **2003**, *43*(2), 143.
- [28] B. K. Kim, S. Y. Park, S. J. Park, *Eur. Polym. J.* **1991**, *27*(4–5), 349.
- [29] L. Piergiovanni, S. Limbo, *Food packaging*, Milan: Springer-Verlag Italy, **2010** Ch.4.
- [30] K. K. Mokwena, J. Tang, *Crit. Rev. Food Sci. Nutr.* **2012**, *52*(7), 640.

**How to cite this article:** A. Visco, C. Scolaro, A. Torrisi, L. Torrisi, *Polym. Cryst.* **2021**, e10207. <https://doi.org/10.1002/pcr2.10207>